様　式　Ｃ－１９、Ｆ－１９－１、Ｚ－１９　（共通）

科学研究費助成事業　　研究成果報告書

令和　３ 年　 ６ 月　 ８ 日現在

機関番号：１７１０４
研究種目：研究活動スタート支援
研究期間：2020～2020
課題番号：２０Ｋ２２３９９

研究課題名（和文）A novel chip-based device to estimate effective wetting area of a single fine droplet at structured surfaces

研究課題名（英文）A novel chip-based device to estimate effective wetting area of a single fine droplet at structured surfaces

研究代表者

張　徳建（Zhang, Dejian）

九州工業大学・大学院工学研究院・博士研究員

研究者番号：１０８７８５０７

交付決定額（研究期間全体）：（直接経費）　　1,100,000円

研究成果の概要（和文）：本研究では，電気化学インピーダンス測定による単一液滴の固液界面の濡れ状態に応じた界面有効濡れ面積の評価を試み，電気化学等価回路による固液界面の接触面積の割合を見積もる方法を確立した．この方法を用いて，従来計測困難である疎水性固液界面の有効接触面積を定量的に評価することができる．また，単一液滴の固液界面の有効接触面積を電気化学インピーダンスと濡れの同時測定を試みた．

研究成果の学術的意義や社会的意義
液滴の固体・液体・気体の異相間接触によって生じた界面抵抗は，液滴寸法が小さくなるとその効果が相対的に増加するため，ナノテクノロジーでは重要な役割を果たす．本研究では，界面抵抗が液滴の固液界面有効濡れ面積に比例することに着目し，固液気の異相間界面抵抗と濡れ・電気化学特性との相関関係を解明することより界面抵抗を定量的に評価することに成功した．マイクロ・ナノデバイスの熱問題を解決するとともに，熱の根源的な理解から次世代省エネルギー技術に貢献する．

研究成果の概要（英文）：The purpose is to estimate the effective wetting area of a single fine droplet at the structured surface quantitatively because the effective wetting area of a solid-droplet system is still an open question. A detection device of an in situ miniaturization electrochemical impedance measurement system is proposed in this study to estimate the effective wetting area of a single fine droplet on the structured surface (apparent flat surface) based on both wettability analysis and impedance analysis.

研究分野：表面科学

キーワード：濡れ　液滴　電気化学インピーダンス　固液界面　有効濡れ面積

１．研究開始当初の背景

Effective wetting area is the real contact area between liquid and solid, which is the key parameter to evaluate the energy transport at the solid–liquid interface. So far, quantitative estimation of effective wetting area of a single fine droplet on the structured surface is a scientific challenging topic, especially for the simultaneous measurement of contact angle and effective wetting area. Considering a droplet on the structured surface as shown in Fig. 1, the wetting state can be either fully wetted, partial wetted or non-wetted, resulting in the significant difference between the effective wetting area and the apparent solid–liquid contact area. Although optical techniques have been applied to visualize the wetting state inside of the structures (Sakai, et al., *Langmuir*, 2009; Daniel, et al., *Nature Physics*, 2017), these methods only can be applied to the transparent substrates and the visualization inside nano/microstructures is quite difficult. On the other hand, we have proposed a theoretical model for the intermediate wetting state (i.e. partial wetting state) at the structured surface and estimated the effective wetting area at the solid–liquid interfaces using the electrochemical impedance measurement system.

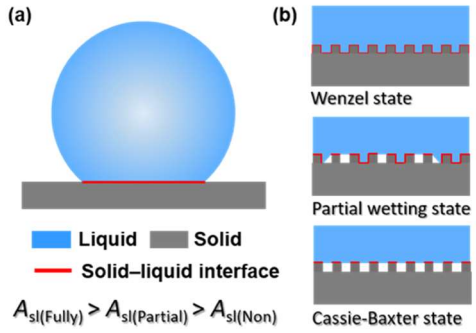

Fig. 1 Schematics of wetting area at solid–liquid interface: (a) macroscopic image of a droplet on the solid surface; (b) microscopic image of wetting states at the solid–liquid interface.

２．研究の目的

The purpose is to estimate the effective wetting area of a single fine droplet at the structured surface quantitatively because the effective wetting area of a solid–droplet system is still an open question. A detection device of an in situ miniaturization electrochemical impedance measurement system is proposed in this study to estimate the effective wetting area of a single fine droplet on the structured surface (apparent flat surface) based on both wettability analysis and impedance analysis.

３．研究の方法

(1) Fabrication and characterization of surfaces

1) Commercial aluminum (1000) pieces with the size of 10 mm × 10 mm were cleaned in acetone, ethanol and deionized water sequentially in a ultrasonic bath.
2) Nano/microstructured Al surfaces were obtained by immersing Al substrates into 1 M $CuCl_2$ solution, followed by a ultrasonic bath cleaning in deionized water.

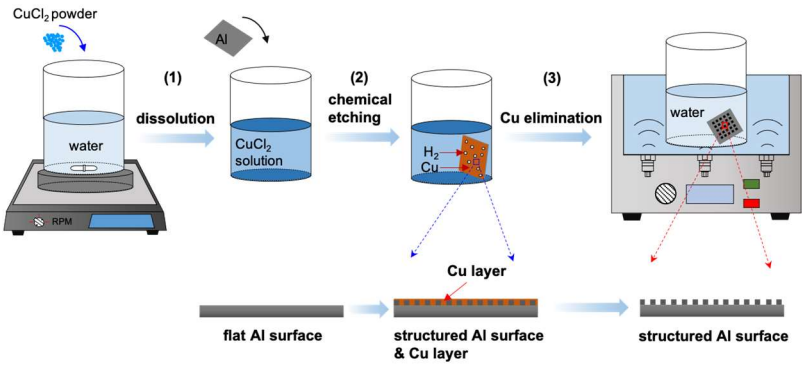

Fig. 2 Schematics of fabrication process for structured Al surfaces.

3) The surface morphology of structured Al surfaces were analyzed by CLSM and SEM images.

(2) Wettability analysis

Measure the water contact angle (WCA) of the fabricated Al surfaces. The measurement system was a transparent box to cover the droplet and the substrate to prevent contaminant adsorption during measurement (Fig. 3). A digital temperature-humidity sensor was put inside to confirm if the local temperature and humidity were constant during the measurement.

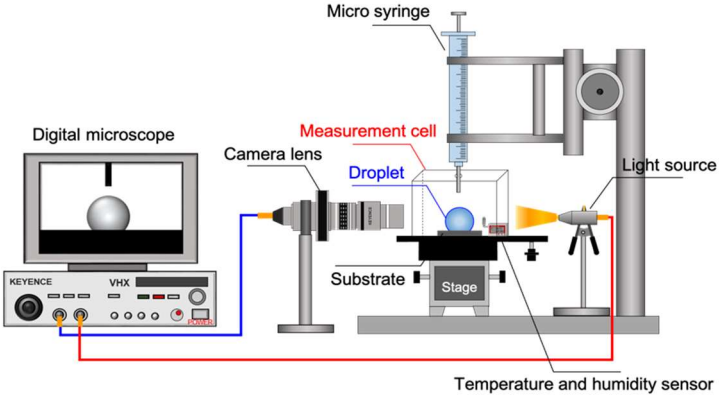

Fig. 3 Water contact angle measurement system.

(3) Electrochemical impedance analysis

The original electrochemical measurement cell is a typical system as shown in Fig. 4, limited to the independent impedance measurements from the experimental system for the wettability measurements. The mean hydrostatic pressure P acted to the surfaces corresponding to a fixed immersing height h is approximately to $P = \rho gh$. As a known problem of this electrochemical system, the pressure difference at solid–liquid interface between the impedance and wettability measurements will cause the deviations of the estimated effective wetting areas. That is, the effective wetting area will increase due to the wetting transition (caused by the imposed pressure).

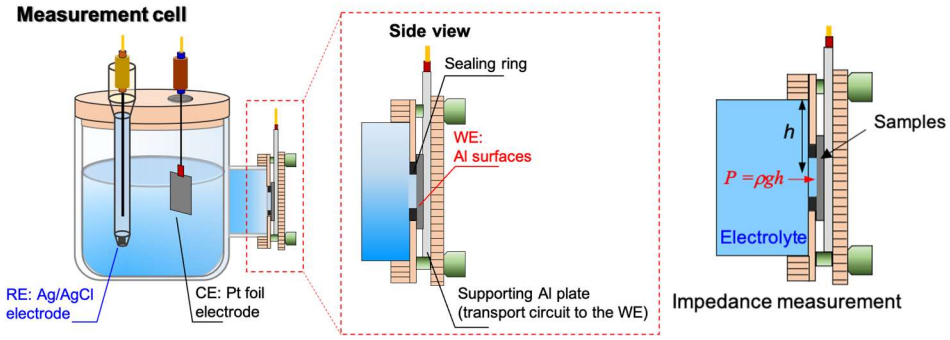

Fig. 4 Original electrochemical impedance measurement system and pressure analysis at the electrolyte-surface interface.

Simultaneous measurements of the impedance and the wettability are necessary to overcome this limitation. However, an electrochemical impedance system for a single fine droplet on a substrate is still a challenging work. The imposed pressure thus results in an increased effective wetting area at solid–liquid interface and the effective wetting area of the impedance results was larger than that of the wettability results. In our experiment, we improved the electrochemical impedance measurement system to make sure the simultaneous measurements of impedance and wettability. Thus, thin solid Ag/AgCl reference electrode is necessary for the single fine solid–droplet surface electrochemical impedance measurement system. Figure 5 shows the preparation procedure for the solid Ag/AgCl reference electrode. To fabricate Ag/AgCl microwire, the pre-cleaned Pt wire (0.2 mm in diameter) was dipped into Ag/AgCl ink then dried at room temperature for 20 h. The schematic of updated electrochemical impedance measurement system is shown in Fig. 6.

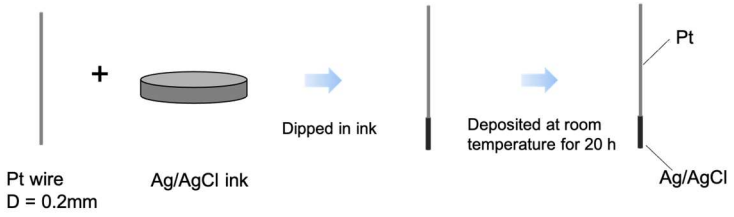

Fig. 5 Scheme employed to prepare solid Ag/AgCl microwire.

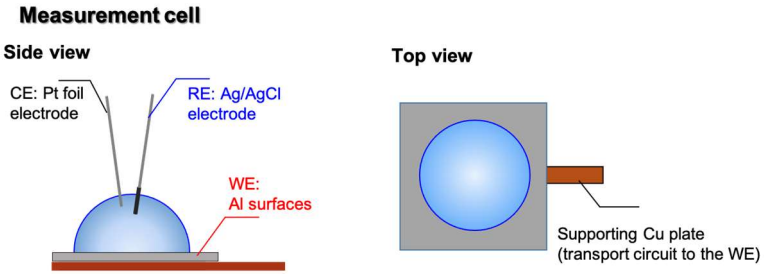

Fig. 6 Improved electrochemical impedance measurement system.

４．研究成果

(1) Surface morphology and wettability analysis

Figure 7 shows the surface morphology images of samples etched for 0 s, 2 s and 10 s, respectively. Polishing trace is easily observed on the bare Al surface. After chemical etching process, porous layer containing nano/microstructures is found at the Al surfaces in Fig. 7 (a2, b2 and a3, b3). Furthermore, the surface cross-sectional profile also indicate that the surface roughness is increased with the increasing etching time, which results in denser nano/microstructures.

WCA has been measured at the Al sample surfaces using a 4μl water droplet. The side views of the droplet are also shown in Fig. 7. WCA at the bare Al surface is 72 ± 1°and the surface hydrophilicity is enhanced with increasing chemical etching time. WCA is 30 ± 2° for surface etched for 2 s and 5 ± 1° for sample etched for 10 s. The droplet images show that the WCA decreases with increasing etching time, while the contact radius increases in an opposite way.

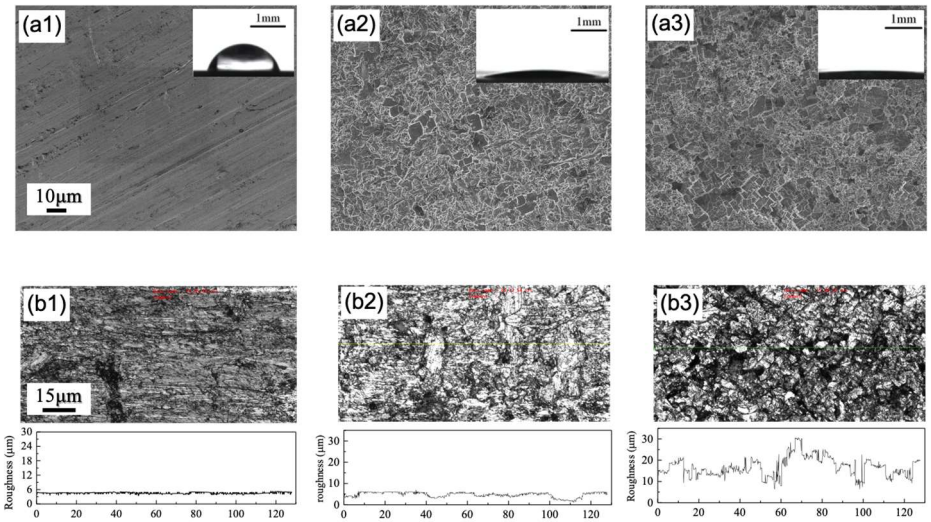

Fig. 7 SEM images, CLSM images and corresponding surface cross-sectional profiles of Al surfaces etched for (a1, b1) 0s, (a2, b2) 2s and (a3, b3) l0 s. The insets show droplets on the surfaces.

(2) Electrochemical impedance analysis

1) Verification of solid Ag/AgCl electrode performance

An electrochemical workstation (Biologic-SP-200) was operated with a three-electrode system (Fig. 8) in a 3.5 wt% NaCl solution at ambient temperature. The system comprised apparent flat Al sample with a 1 cm^2 exposed surface area as the working electrode, a platinum foil with a 4 cm^2 as the counter electrode, classical Ag/AgCl and solid Ag/AgCl were used as the reference electrode. The measurement was conducted by immersing the substrate vertically in a bulk liquid electrolyte. Electrochemical impedance spectroscopy (EIS) was carried out with a 10 mV sinusoidal signal in a frequency range from 100 kHz to 100 mHz.

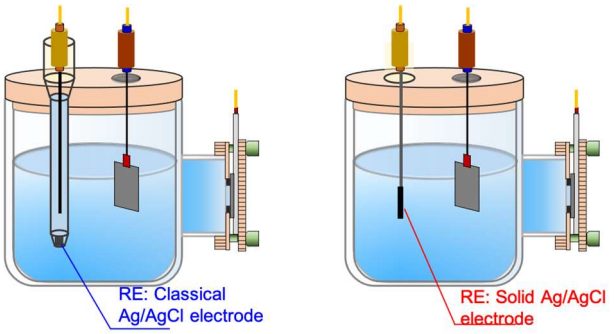

Fig. 8 Classical and solid Ag/AgCl reference electrode system.

The typical Nyquist plots for Al surfaces with classical and solid reference electrodes are shown in Fig. 9, representing the impedance as a complex number with its real part in x-axis and the imaginary part in y-axis. The semicircles in the Nyquist plots indicate the effect of double-layer capacitance. We can observe that the capacitive arc diameters for the Al surfaces with difference reference electrodes are almost similar with each other. To evaluate the electrochemical parameters from the measured impedance spectra, schematic of the solid–liquid interface and one-time constant equivalent electrical circuit (EEC) was used to fit the obtained Nyquist results, as shown in the inset of Nyquist plots. During the EEC fitting for the Al surface, we used R_s, R_{ct}, and C_{dl} to denote the solution resistance, charge transfer resistance, and double-layer capacitance, respectively. As defects cannot be avoided on the Al surface, capacitors often do not exhibit ideal capacitive behavior. Therefore, we applied the constant phase element (CPE) to determine the non-ideal frequency-dependent properties of C_{dl}. The obtained electrochemical parameters, including R_s, R_{ct}, and CPE, are listed in Table 1. Generally, charge transfer resistance is more clearly

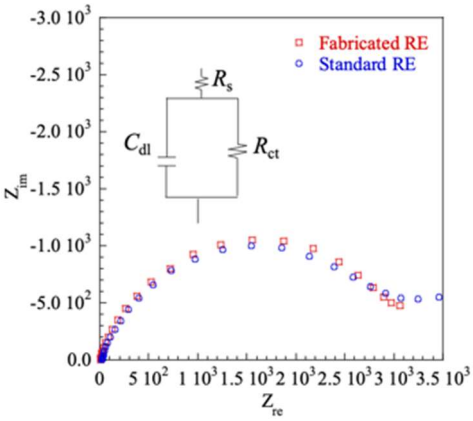

Fig. 9 Nyquist plots for the standard RE and fabricated RE. The inset is EEC for Nyquist fitting.

Table 1. Electrochemical data for samples fitted based on the EECs.

	R_s	CPE		R_{ct}
	($\Omega \cdot cm^2$)	Q (Ω^{-1} s^{-n}/cm^2)	n	($\Omega \cdot cm^2$)
Solid RE	11.01	3.21×10^{-5}	0.81	3.0×10^3
Classical RE	21.94	2.78×10^{-5}	0.77	3.1×10^3

represents electrochemical properties of the measured surfaces. We found that the fitted R_{ct} for the fabricated solid Ag/AgCl RE is 3000 Ω·cm^2 which is almost equal to that of classical Ag/AgCl RE (3100 Ω·cm^2). The results indicate that the fabricated solid Ag/AgCl RE is verified and can be used for the electrochemical impedance measurement.

2) Comparison between classical and single droplet electrochemical impedance measurement system

The electrochemical responses of this single fine solid–droplet surface system were compared to those obtained with a classical electrochemical measurement system. As shown in Fig. 10a, the classical cell comprised deionized water as electrolyte, apparent flat Al surface with a 1 cm^2 exposed surface area as the working electrode, a platinum foil with a 4 cm^2 as the counter electrode, classical Ag/AgCl used as the reference electrode. Different from the classical cell, the droplet cell (Fig. 10b) includes Pt wire, solid Ag/AgCl microwire, and 10 μl deionized water droplet was used as CE, RE and electrolyte, respectively.

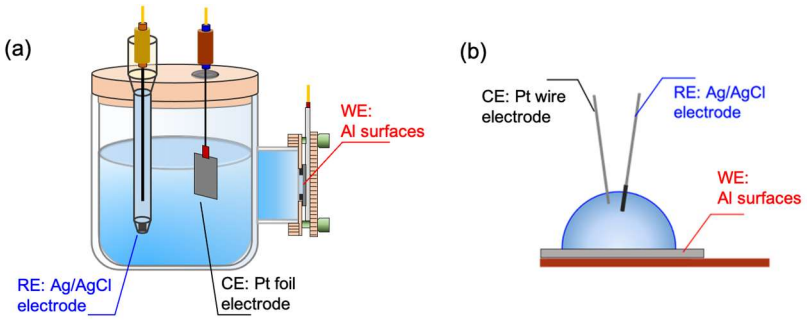

Fig. 10 Electrochemical impedance measurement system: (a) classical cell, (b) single droplet cell.

EIS was utilized to analyze the interfacial electrical impedance of samples. The typical Nyquist plots for the samples in deionized water were shown in Fig. 11. We can clearly find that there are two-time constant in the measured Nyquist plots. Thus, we use two-time constant EEC to fit the obtained Nyquist results. The fitted electrochemical parameters, including R_s, R_1, R_2, CPE_1 and CPE_2, are listed in Table 2. We can find that the fitted R_1 in the classical cell is 3.1 × 10^4 Ω·cm^2, which agrees with that in the droplet cell (3.2 × 10^4 Ω·cm^2) in general. However, there is an extra loop exists between the first and second capacitive impedance loop in the droplet cell measurement. Moreover, compare to the Nyquist plot of the classical cell, the second capacitive impedance loop in the droplet cell measurement is larger, resulting in a larger $R_{2\text{-droplet}}$ (7.9 × 10^4 Ω·cm^2) than $R_{2\text{-classical}}$ (4.3 × 10^4 Ω·cm^2).

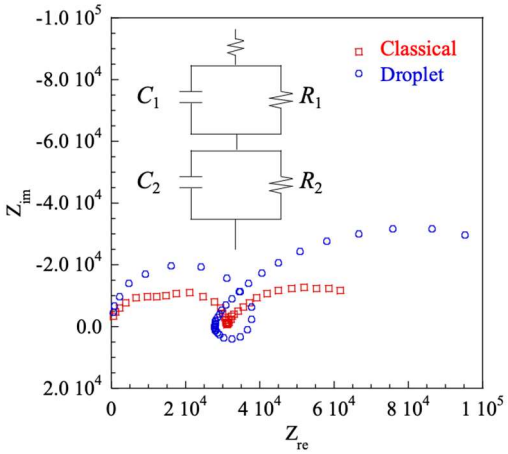

Fig. 11 Electrochemical impedance results: (a) Nyquist plots; (b) Equivalent electrical circuits for Nyquist fitting.

Table 2. Measured electrochemical parameters in different temperature.

	R_s (Ω.cm^2)	CPE_1		CPE_2		R_1 (Ω.cm^2)	R_2 (Ω.cm^2)
		Q (Ω^{-1} s^{-n}/cm^2)	n	Q (Ω^{-1} s^n/cm^2)	n		
Classical	4.8 × 10^2	5.08 × 10^{-10}	0.85	1.4 × 10^{-5}	0.67	3.1 × 10^4	4.3 × 10^4
Droplet	1.7 × 10^3	3.37 × 10^{-11}	1	7.4 × 10^{-6}	0.85	3.2 × 10^4	7.9 × 10^4

3) Future works

The impedance results of the droplet cell agree with the classical cell in general. However, there are still few limitations of the proposed method. One is the difficulty to measure the electrochemical impedance of superhydrophilic surfaces. During the impedance measurement in droplet cell, there should be a certain height of a droplet to ensure the CE and RE can be dipped into. Thus, we use apparent flat Al surface as main experimental samples in this study. Another unclear point is the existence of extra loop between two capacitive impedance loops. Further investigation on the impedance measurement of superhydrophilic surfaces and the reason of extra loop is required.

５．主な発表論文等

〔雑誌論文〕　計0件

〔学会発表〕　計1件（うち招待講演　0件／うち国際学会　1件）

１．発表者名 Dejian ZHANG
２．発表標題 Effective wetting area at hydrophobic surface based on electrochemical impedance analysis
３．学会等名 8th Symposium on Applied Engineering and Science（国際学会）
４．発表年 2020年

〔図書〕　計0件

〔産業財産権〕

〔その他〕

―

６．研究組織

	氏名 （ローマ字氏名） （研究者番号）	所属研究機関・部局・職 （機関番号）	備考

７．科研費を使用して開催した国際研究集会

〔国際研究集会〕　計0件

８．本研究に関連して実施した国際共同研究の実施状況

共同研究相手国	相手方研究機関